Severe Accident Scoping Simulations of Accident-Tolerant Fuel Concepts for BWRs

M3FT-15OR0202333

K. R. Robb*
Oak Ridge National Laboratory, P.O. Box 2008, Oak Ridge, TN 37830, USA
robbkr@ornl.gov

1. INTRODUCTION

Accident-tolerant fuels (ATFs) are fuels and/or cladding that, in comparison with the standard uranium dioxide (UO_2)–Zircaloy system, can tolerate loss of active cooling in the core for a considerably longer time period while maintaining or improving the fuel performance during normal operations [1]. It is important to note that the currently used UO_2–Zircaloy fuel system tolerates design basis accidents (and anticipated operational occurrences and normal operation) as prescribed by the US Nuclear Regulatory Commission.

Previously, preliminary simulations of plant response have been performed under a range of accident scenarios using various ATF cladding concepts and fully ceramic microencapsulated fuel. Design basis loss of coolant accidents (LOCAs) and station blackout (SBO) severe accidents were analyzed at Oak Ridge National Laboratory (ORNL) for boiling water reactors (BWRs) [2]. Researchers have investigated the effects of thermal conductivity on design basis accidents [3] and investigated silicon carbide (SiC) cladding [4], as well as the effects of ATF concepts on the late-stage accident progression [5]. These preliminary analyses were performed to provide initial insight into the possible improvements that ATF concepts could provide and to identify issues with respect to modeling ATF concepts. More recently, preliminary analyses for a range of ATF concepts have been evaluated internationally for LOCA and severe accident scenarios for the Chinese CPR1000 [6] and the South Korean OPR-1000 pressurized water reactors (PWRs) [7]. In addition to these scoping studies, a common methodology and set of performance metrics were developed to compare and support prioritizing ATF concepts [8].

This work focuses on a proposed ATF concept based on iron-chromium-aluminum alloys (FeCrAl) [9, 10]. With respect to enhancing accident tolerance, FeCrAl alloys have substantially slower oxidation kinetics than the zirconium alloys that are typically employed. During a severe accident, FeCrAl would tend to generate heat and hydrogen from oxidation at a slower rate than the zirconium-based alloys in use today.

The previous study of the FeCrAl ATF concept during SBO severe accident scenarios in BWRs [2] was based on simulating short-term SBO (STSBO), long-term SBO (LTSBO), and modified SBO scenarios occurring in a BWR-4 reactor with MARK-I containment. The analysis indicated that FeCrAl had the potential to delay the onset of fuel failure by a few hours, depending on the scenario, and it could delay

lower head failure by several hours. The analysis demonstrated reduced in-vessel hydrogen production. However, the work was preliminary and was based on limited knowledge of material properties for FeCrAl. Limitations of the MELCOR code were identified for direct use in modeling ATF concepts. This effort used an older version of MELCOR (1.8.5). Since these analyses, the BWR model has been updated for use in MELCOR 1.8.6 [15], and more representative material properties for FeCrAl have been modeled. Sections 2–4 present updated analyses of the FeCrAl ATF concept response during severe accidents in a BWR. The purpose of the study is to estimate the potential gains afforded by the FeCrAl ATF concept during BWR SBO scenarios.

In addition to the updated FeCrAl analyses documented in Sections 2–4, a parametric study in MELCOR was attempted. The goal of the study was to identify which fuel, cladding, and structure property changes provide the best potential improvements for delaying or mitigating severe accidents. However, the integral nature of severe accidents coupled with on/off failure modes, strong dependence on timing, and regime dependent phenomena resulted in difficult to interpret results. The parametric study is further discussed in Appendix A.

2. ANALYSIS SETUP

Severe accident simulations were performed modeling the FeCrAl ATF concept, and the results for key figures of merit were compared against baseline results using the traditional UO_2–Zircaloy system. The following describes the accident scenarios chosen, the figures of merit used in the comparison, the MELCOR code, the plant model, and the modeling of FeCrAl in MELCOR.

2.1. Accident Scenario and Figures of Merit

The SBO severe accident scenario was chosen for investigation. During the SBO scenario, the reactor is assumed to successfully trip (reference time 0 h). All alternating current (AC) power, including off-site and on-site power (diesel generators), is assumed to be lost at 0 h. The timing of the loss of direct current (DC) power (batteries) was varied in the scenarios from 0 h (STSBO) to 4 h and 8 h. Traditionally, loss of DC power was assumed to occur in the 4–8 h window, and the scenario was termed as the long-term station blackout (LTSBO). While DC power is maintained, the reactor core isolation cooling (RCIC) system and/or the high-pressure coolant injection (HPCI) system can be used to inject cooling water into the primary system. After the loss of DC power, the ability to inject water ceases. Two different water injection recovery scenarios were considered. In one scenario, water injection into the primary system is not restored (unmitigated SBO). In the other scenario, water injection is restored into a feedwater line at a rate of 0.568 m^3/min (150 GPM) 8 h after the loss of DC power (mitigated SBO). This injection rate is sufficient to offset the decay heat. In these scenarios, it was assumed that operators did not take action (or that they were unable to take action) to depressurize the reactor pressure vessel (RPV) or containment. All simulations were specified to end 32 h after reactor shutdown.

The SBO scenario was chosen due to its high contribution to the overall core damage frequency for BWRs [12, 13]. In addition, the accidents that occurred at Fukushima Daiichi Units 1–3 were variants of the traditional STSBO and LTSBO scenarios [14]. Key figures of merit, provided in Table I, were defined related to the timing of the accident progression and flammable gas generation.

Table I. Figures of merit descriptions.

Figure of merit		Significance
Timing	0.5 kg of H_2 is generated	Onset of hydrogen generation
	First fuel failure (cladding gap release)	First release of radionuclides from fuel
	100 kg of H_2 is generated	Significant combustible gas generated
	First cladding melting	Degradation of coolable geometry
	Lower head failure	Escalation of accident to ex-vessel
	Containment failure	Loss of radionuclide barrier
	First deflagration in building	Escalation of accident
	0.5 kg of noble gas release to environment	Onset of radionuclide release to outside
Total mass	H_2 gas generated by end of simulation	Flammable gas potential
	CO gas generated by end of simulation	Flammable gas potential

2.2. Overview of Tools

MELCOR is a system-level code that models the progression of severe accidents in light water nuclear power plants. It was developed and has been maintained by Sandia National Laboratories for the US Nuclear Regulatory Commission. The code encompasses various phenomena that can occur during a severe accident, including the thermal-hydraulic response; the heat up, degradation, and relocation of the core material; transport of radionuclides; and hydrogen generation and combustion. MELCOR is primarily used to estimate the source term from severe accidents. MELCOR version 1.8.5 was released in 2000 [11]; version 1.8.6 was released in 2005 [15]; and version 2.1 was released in 2008 [16].

Previous preliminary simulations [2] of the FeCrAl ATF concept were performed using MELCOR 1.8.5. A number of modeling improvements were incorporated into version 1.8.6. One key modeling change was the treatment of the reactor vessel bottom head [15]. MELCOR version 1.8.6 is still widely used internationally. From version 1.8.6 to 2.1, the major code improvements were primarily related to the code internal structure, although changes were also made to the code input structure. In this study, MELCOR version 1.8.6(.4073), as compiled by ORNL personnel using the Intel 11.1.064 compiler, is used on a Linux-based computer with Intel-based hardware. A few minor source code changes were required to model FeCrAl; they are discussed in Section 2.3.

2.3. Plant Model Description

The MELCOR plant model used is for Peach Bottom (Unit 2 or 3), a BWR series 4 (BWR/4) with a Mark I containment. The model includes all major components, including the reactor; containment; reactor building; and various cooling systems (pumps, sprays, piping, tanks), as well as system and scenario control logic. The model was recently updated from MELCOR 1.8.5 for use in MELCOR 1.8.6. This update, the model's lineage, and additional model updates have been previously described [17].

Within the model, there are different competing failure modes for various structures in the system. Minor differences in the accident progression (i.e., due to material properties) may result in a different failure mode. Differences in failure modes can cause simulations to vary more substantially from one another. The following paragraphs summarize the available competing failure modes that are modeled for some of the components of interest.

There are three competing modes modeled for lower head failure: thermal failure of a penetration due to high temperature of a penetration or the lower head, lower head yielding via creep-rupture, and RPV over-pressurization. The over-pressurization failure mode will not occur during the accident scenarios

selected. Therefore, there is a competition between failure of a penetration due to high temperature and yielding of the lower head.

There are four competing failure modes of the containment modeled. Three are functions of pressure and local temperature; they include rupture of the wetwell, rupture of the drywell liner, and leakage of the drywell head flange. The final mode is melt-through of the drywell liner due to contact with molten core materials. Each failure mode opens a unique release path for radionuclides and combustible gases into the reactor building.

2.4. Modeling FeCrAl ATF concept in MELCOR

The FeCrAl material was modeled in MELCOR by replacing the material properties for the Zr and ZrO_2 materials with those of FeCrAl and FeCrAl oxide. The thermophysical properties for metallic FeCrAl were modeled after Kanthal APM and are the same as those used previously for LOCA analyses [2], as illustrated in Figure 1. The high temperature properties were linearly extrapolated to 2000 K from the available data and held constant for temperatures above 2000 K. The oxide properties were modeled as independent of temperature, as shown in Table II. The appropriate thermophysical properties as functions of temperature for bulk oxidized FeCrAl need to be refined in the future. The formation of eutectics greatly influences the core degradation process in the existing reactors that use Zircaloy [18]. The potential eutectic formation of FeCrAl with B_4C, Inconel, and UO_2 was not modeled and needs to be investigated in the future.

Table II. Material properties for FeCrAl and FeCrAl Oxide.

Assumed material properties	FeCrAl	FeCrAl Oxide
Melting point (K)	1,773	1,901
Heat of fusion (J/kg)	275,000	687,463
Density (kg/m^3)	Kanthal APM (Figure 1)	5,180
Thermal conductivity (W/m K)		4.0
Specific heat (J/kg K)		900.0

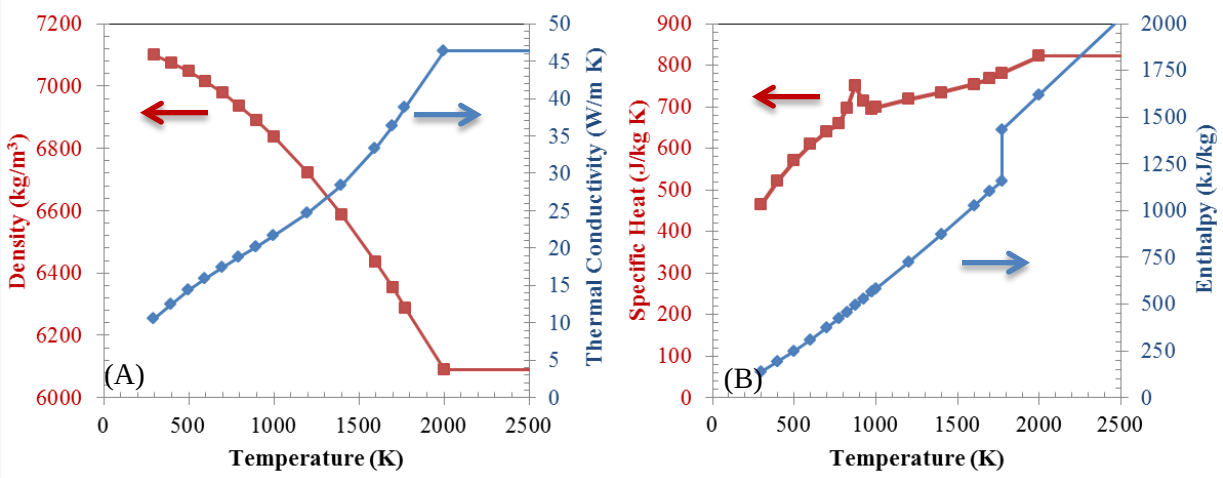

Figure 1. Modeled FeCrAl properties: density and thermal conductivity (A); specific heat and enthalpy (B).

The oxidation kinetics of FeCrAl with steam while in vessel was modeled by Eq. (1) based on experimental data reported in Ref. [19], where K(T) is the oxidation rate constant and T is temperature. The oxidation kinetics of FeCrAl with oxygen while in vessel were based on the kinetics of Zircaloy

reaction with oxygen but reduced by three orders of magnitude. However, the reaction of FeCrAl with O_2 has limited importance during in-vessel core degradation for the scenarios chosen.

$$K(T)=\left(784.0\ \frac{kg^2}{m^4\ s}\right)\cdot \exp\left(\frac{-41376.0\ K}{T}\right) \quad (1)$$

The heat of oxidation for zirconium- and steel-based materials is hardcoded in MELCOR. To more accurately reflect the FeCrAl material, the heat of oxidation for reaction with H_2O and O_2 was modified in the MELCOR source code. The modification was performed to reflect FeCrAl comprised of 73 wt % Fe-22Cr-5Al with production of Fe_3O_4, Cr_2O_3 and Al_2O_3 oxides. The heat of reaction (at 298 K) for FeCrAl was taken to be 1.247 MJ/kg for reaction, with H_2O and 8.837 MJ/kg for reaction with O_2. Also, the oxidation reaction equation for MELCOR's Zr material was modified to reflect the stoichiometry of oxidizing FeCrAl.

When switching from Zircaloy to FeCrAl, the cladding thickness was reduced by 50% while maintaining the cladding outer diameter. This resulted in 43% less cladding material mass than in the base case. The channel box dimensions remained constant. The gap between the fuel pellet and the cladding was assumed to be zero in both the UO_2-FeCrAl and the UO_2-Zircaloy models. The fuel pellet outer diameter was increased to correspond to the reduction in cladding thickness. This resulted in the UO_2 mass increasing by 18.5%. The reduction in cladding thickness is based on previous reactor physics assessments of FeCrAl cladding in PWRs in which it was determined that maintaining operational cycle lengths was best accomplished through a small increase in batch-average enrichment and reduction of the cladding thickness to about half of the nominal thickness [20, 21]. Recent neutronics studies found similar results for BWRs as well; however, the studies suggest reducing both the cladding and channel box thicknesses by about 50% [22, 23].

The core radionuclide inventory and distribution and the total decay heat and distribution were not modified and were the same as the model with Zircaloy cladding. To date, a reference assembly design has not been developed that can accommodate the integral considerations of thermal hydraulics, neutronics, fuel performance, and economics. Once a fuel assembly design is developed, the gains afforded by the FeCrAl ATF concept during severe accidents should be revisited.

The core-concrete interaction modeling in MELCOR is performed by a separate package (based on CORCON-Mod3) with its own material properties. During transfer of melt from in-vessel to ex-vessel, the model was modified to map the Zr and Zr oxide materials (modified to model FeCrAl) to stainless steel and stainless steel oxide materials. Thus, the FeCrAl material is treated as stainless steel by the core-concrete interaction modeling. Some insight into the consequences of this can be found in Ref. [5]. Substituting stainless steel (or Zr) for FeCrAl in the ex-vessel modeling could affect the oxidation rate of the material; however, the oxidation rate is generally limited by the availability of concrete decomposition gases. The substitution affects the amount of energy generated during oxidation, as well as the amount of hydrogen generated. The substitution will also affect the material properties predicted for the debris. This limitation could be explored and addressed in the future, but it is likely overshadowed by the limited ex-vessel debris coolability models that are integrated into MELCOR 1.8.6 and early 2.1 versions [24].

3. ANALYSIS RESULTS

3.1. Unmitigated Station Blackout

3.1.1. Overview of results

Three SBO accident scenarios in which DC power is assumed to be lost at 0, 4, or 8 h and water injection is not recovered (unmitigated), were investigated. For each scenario, a traditional Zircaloy cladding and channel boxes were modeled, as well as for FeCrAl cladding and channel boxes. The figures of merit results for all cases are summarized in Table III.

For all the unmitigated SBO scenarios analyzed, the timing of the accident is delayed in the cases using FeCrAl compared to those employing Zircaloy. Table IV summarizes the difference in the figures of merit between the FeCrAl and Zircaloy cases for each of the three scenarios. Employing FeCrAl compared to Zircaloy improved all the figures of merit except for the two noted in red. The increased time ranges from tens of minutes to a few hours. This provides additional time for operators to perform mitigation actions, for offsite equipment to arrive, and for evacuations of the surrounding area. Substantially less hydrogen is generated in all scenarios, and less carbon monoxide is generated in two of the scenarios. The reduced amount of combustible gases decreases the potential for deflagrations to occur in the reactor building, which could inhibit the accident response. Figure 2 illustrates the additional margin provided by the FeCrAl ATF concept for two key stages of an accident: the onset of cladding melting and relocation, and the onset of radionuclide release to the environment.

Table III. Figure of merit results for unmitigated station blackout simulations.

Figure of merit	Scenario results: DC failure					
	0 h		4 h		8 h	
	Zirc	*FeCrAl*	*Zirc*	*FeCrAl*	*Zirc*	*FeCrAl*
0.5 kg of H_2 is generated[a]	70	109	538	602	740	811
First fuel failure (gap release)[a]	72	76	543	551	746	755
100 kg of H_2 is generated[a]	97	182	584	752	791	980
First cladding melting[a]	112	223	622	800	827	1,034
Lower head failure[a]	568	553	1,199	1,237	1,387	1,512
Containment failure[a]	582	628	1,076	1,315	1,250	1,515
First deflagration in building[a]	582	629	1,076	1,324	1,250	1,525
0.5 kg noble gas release to environment[a]	571	629	1,078	1,316	1,251	1,516
H_2 gas generated by end of simulation[b]	3,164	1,738	2,614	1,049	2,911	844
CO gas generated by end of simulation[b]	40,048	40,858	20,161	13,960	18,488	6,841

[a] = *minute* [b] = *kg*

Table IV. Differences in figure of merit results for Zircaloy and FeCrAl unmitigated SBO simulations.

Figure of merit	Difference between Zircaloy and FeCrAl cases: DC failure		
	0 h	4 h	8 h
0.5 kg of H_2 is generated[a]	39	64	71
First fuel failure (gap release)[a]	4	8	10
100 kg of H_2 is generated[a]	85	169	190
First cladding melting[a]	110	178	207
Lower head failure[a]	-16	38	125
Containment failure[a]	46	239	265
First deflagration in building[a]	47	247	275
0.5 kg noble gas release to environment[a]	59	238	265
H_2 gas generated by end of simulation[b]	-1426	-1565	-2067
CO gas generated by end of simulation[b]	810	-6201	-11647

[a] = *minute* [b] = *kg*

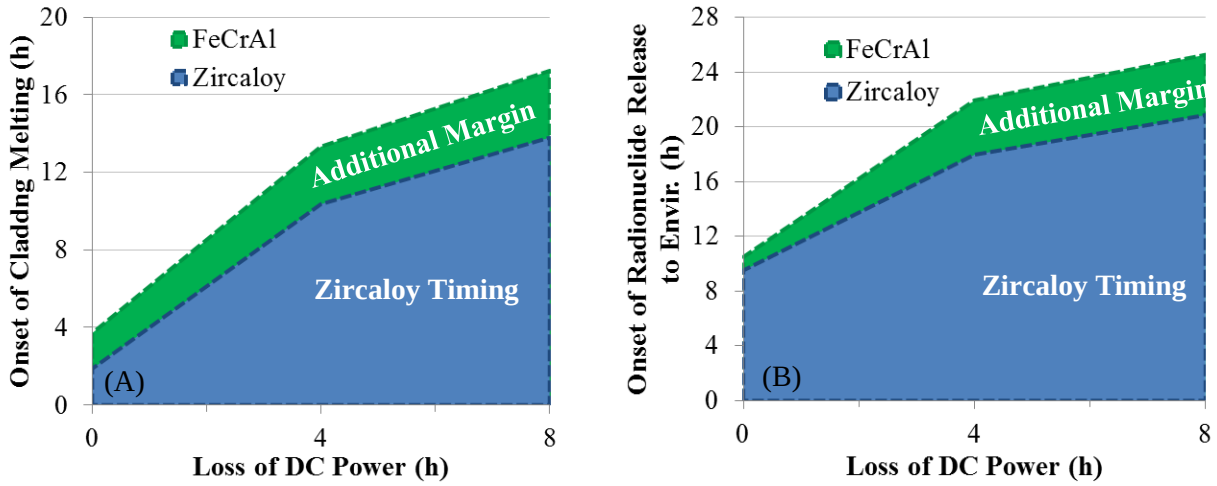

Figure 2. Additional margin to onset of fuel failure (A) and radionuclide release (B) provided by FeCrAl.

3.1.2. Extended discussion of the SBO scenario with loss of DC power at 8 h

The following discussion compares in more detail the results from the Zircaloy and FeCrAl cases for the 8 h SBO scenario (Figure 3–Figure 5). The comparisons of the 0 h and 4 h SBOs are similar, but with shifted timescales.

The early accident progression is nearly identical between cases, as shown in Figure 3 through Figure 5. Both concepts are modeled as having the same radionuclide inventory and therefore having the same decay heat. Thus, the water injection required by the HPCI and RCIC systems, the SRV actuations, and boil-down rate of the cores are very similar. The difference between concepts in the initial stored energy at the time of shutdown has negligible impact given the time interval of interest.

The time until the first cladding failure, releasing the fuel rod gap and plenum contents, is only delayed by 10 min. The temperature at which the fuel cladding is assumed to burst is below the temperature at which oxidation begins to be appreciable. Therefore, the timing of rupture is primarily dependent upon decay heat and is similar for both cases. The effective temperature at which FeCrAl clad will burst depends upon the fuel assembly design and will need to be refined in the future.

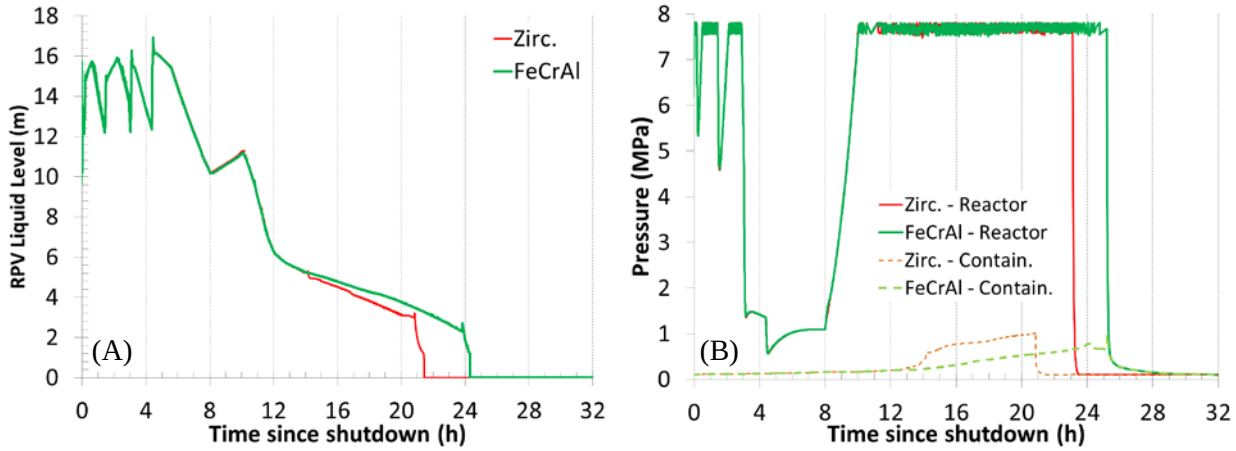

Figure 3. RPV liquid level (A); reactor and containment pressure (B).

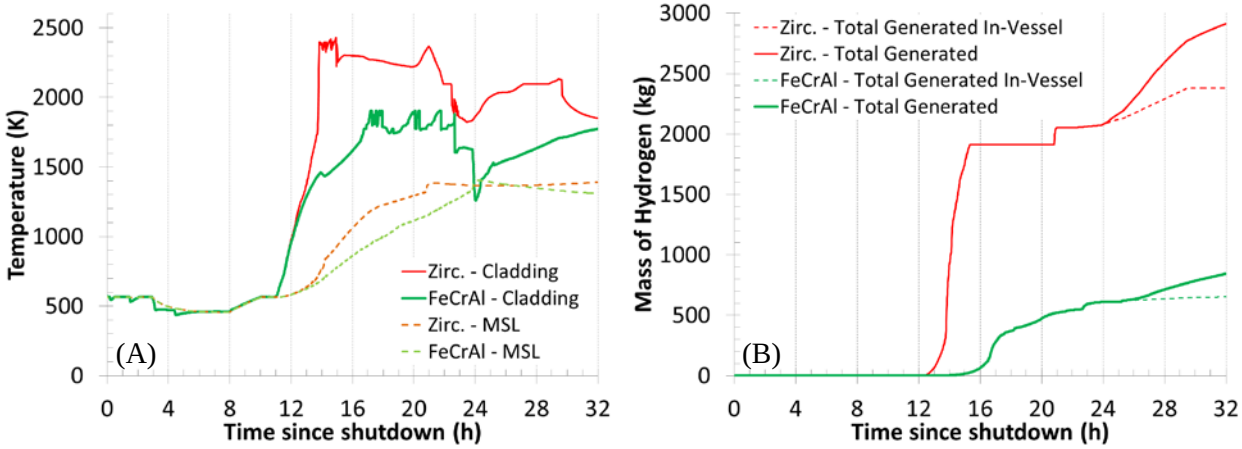

Figure 4. Peak intact cladding and main steam line temperature (A); mass of hydrogen generated (B).

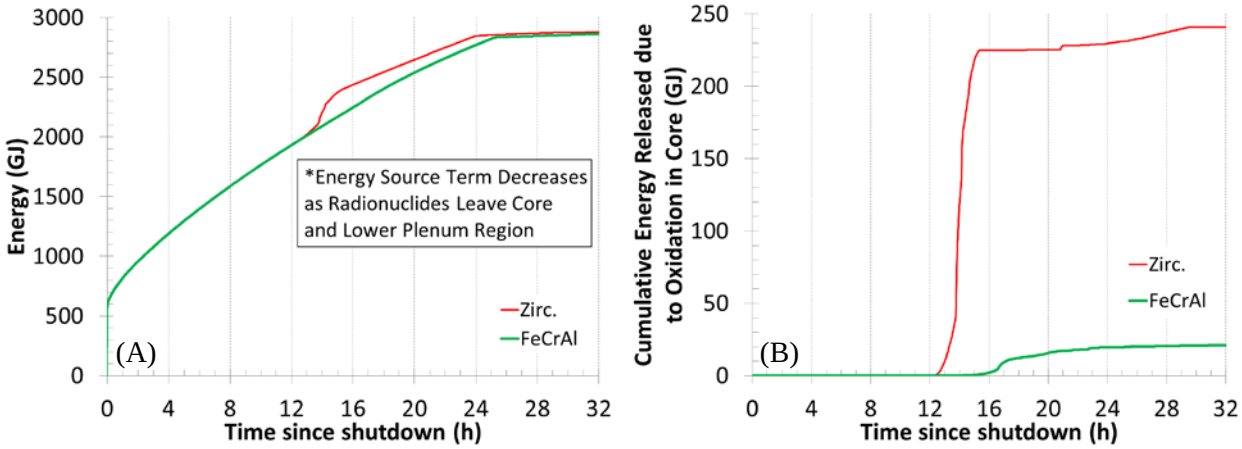

Figure 5. Total cumulative energy generated in core (A); cumulative energy from oxidation in core (B).

The onset of hydrogen generation is delayed by 71 min. The generation of significant quantities (taken to be 100 kg) of hydrogen is delayed by approximately 190 min. This is due to the slower oxidation kinetics

of FeCrAl. The slower kinetics also result in less heat being generated during oxidation in the FeCrAl case (Figure 5). This leads to cooler temperatures in the fuel, the upper structures in the RPV, and in the main steam line (Figure 4A). Note, the temperature reported for the main steam line is the inside surface temperature.

The onset of fuel melting, which degrades the core's coolable geometry, is delayed by 3.5 h. The FeCrAl ATF concept provides 25% more time for mitigation actions to be taken before the core begins losing its coolable geometry. The lower head is predicted to fail only 2.1 h later for the FeCrAl case. The core relocation characteristics can impact the debris configuration in the lower plenum, which affects the timing and failure mode of the lower head. For the Zircaloy case, the lower head is predicted to fail via creep-rupture, whereas a penetration is predicted to fail first in the FeCrAl case. The difference in the predicted failure mode has minor importance given the uncertainty in our knowledge and modeling of lower head failure modes [18, 25].

The drywell head flange is eventually predicted to fail in both cases due to over pressurization of containment. However, containment is over pressurized in the Zircaloy case before failure of the lower head. In contrast, containment fails after lower head failure in the FeCrAl case. The additional heat generated during oxidation of the Zircaloy (Figure 5) causes containment to pressurize sooner than the FeCrAl case (Figure 3B). Also, the additional hydrogen, a non-condensable gas, adds to the containment pressurization. Ultimately, containment failure is predicted to occur approximately 4.4 h later in the FeCrAl case compared to the Zircaloy case. Soon after containment failure, deflagrations are predicted to occur in the reactor buildings for both cases. However, the deflagrations are predicted to occur 4.5 h later in the FeCrAl case. Due to the difference in containment failure timing, the start of radionuclide release to the environment is delayed by approximately 4.4 h between the FeCrAl and Zircaloy cases.

The debris characteristics in the lower plenum and the timing of lower head failure affect the ex-vessel prediction of melt spreading, molten core–concrete interaction (MCCI), and potentially the containment failure modes. The case using FeCrAl results in approximately 20% less melt mass being ejected ex-vessel. This is despite the higher density of FeCrAl compared to Zr and the additional mass of UO_2 in the FeCrAl case. However, the outer ring of assemblies in the FeCrAl case is predicted to remain standing in the core region in contrast to what is predicted to occur in the Zircaloy case. The initial melt ejection occurs at a temperature 150 K hotter in the FeCrAl case than in the Zircaloy case.

The total hydrogen generated during the simulation is 71% less in the FeCrAl case compared to the Zircaloy case. The FeCrAl case produces much less hydrogen in-vessel than the base case (Figure 4B). Once ex-vessel, the rates of hydrogen and carbon monoxide generation are predicted to be slower than in the Zircaloy case. The total carbon monoxide generated (primarily ex-vessel) during the simulation is 63% less in the FeCrAl case compared to the Zircaloy case.

3.2. Mitigated Station Blackout

For the mitigated SBO scenarios, water was injected into the feedwater line at 0.568 m^3/min (150 GPM) starting 8 h after the loss of DC power. This is a sufficient rate to offset the decay heat and refill the RPV. The results for the figures of merit for all cases are summarized in Table V.

Table V. Figure of merit results for mitigated station blackout simulations.

Figure of merit	Scenario results: DC failure					
	0 h		4 h		8 h	
	Zircaloy	FeCrAl	Zircaloy	FeCrAl	Zircaloy	FeCrAl
0.5 kg of H_2 is generated [a]	70	109	538	602	740	811
First fuel failure (gap release) [a]	72	76	543	551	746	755
100 kg of H_2 is generated [a]	97	182	584	752	791	980
First cladding melting [a]	112	223	622	1055	827	1039
Lower head failure [a]	NA	NA	NA	NA	NA	NA
Containment failure [a]	716	NA	NA	NA	1162	NA
First deflagration in building [a]	716	NA	NA	NA	1162	NA
0.5 kg noble gas release to environment [a]	718	NA	NA	NA	1162	NA
H_2 gas generated by end of simulation [b]	1973	534	1879	317	1919	355

[a] = *minute* [b] = *kg*

NA: Not applicable, was not predicted to occur for that case

In all cases, the water addition occurs in time to prevent lower head failure. However, in two of the cases employing Zircaloy, the containment is predicted to fail with subsequent deflagrations occurring in the reactor building and release of radionuclides. As noted in Section 2.2, there are multiple containment failure modes. The failure and leakage of the containment's drywell head is modeled to depend on the temperature of the head and the drywell pressure. Figure 6 compares the predicted drywell head temperature and drywell pressure over the course of the accident (up to 32 h) to the failure limit modeled for the drywell head. As shown, the drywell head fails in the Zircaloy case with loss of DC at 8 h. For the Zircaloy case with loss of DC at 0 h, the wetwell actually fails just before drywell failure. Finally, due to minor differences in the core degradation process, the Zircaloy case with loss of DC at 4 h is not predicted to fail containment. However, the predicted containment conditions are close to the modeled failure criteria. In contrast to the Zircaloy cases, the decreased heat load on containment from oxidation of the FeCrAl cladding and channel boxes as well as the reduction in non-condensable gases in containment result in much lower containment pressures over time.

In general, the accident cases employing the FeCrAl ATF concept are stabilized before lower head failure, containment failure, or any external radiological release. This is in contrast to the cases employing Zircaloy, where the accident progresses further, containment loads are higher, and radiological releases are predicted for two of the cases.

Significantly less hydrogen, approximately 1.5 tons, is generated in the cases employing the FeCrAl ATF concept compared to the Zircaloy cases. This hydrogen stays inside the inerted containment for the FeCrAl cases, whereas the hydrogen leaks into the containment building and deflagrates in the Zircaloy cases. Note, for both scenarios, negligible amounts of CO were predicted to be generated. The deflagrations that took place during the accidents at Fukushima Daiichi inhibited the ability of the operators to stabilize the accidents [14]. In the scenarios simulated, water injection is restored 8 h after DC failure and maintained regardless of deflagrations occurring in the reactor building. Given the experiences at Fukushima Daiichi, the deflagrations that are predicted to occur in the Zircaloy cases could result in further delaying or in inhibiting the ability to maintain water injection than is captured in the scenarios simulated.

These results illustrate the increased potential to stabilize a severe accident at a reactor using a FeCrAl ATF concept compared to one employing the traditional Zircaloy system.

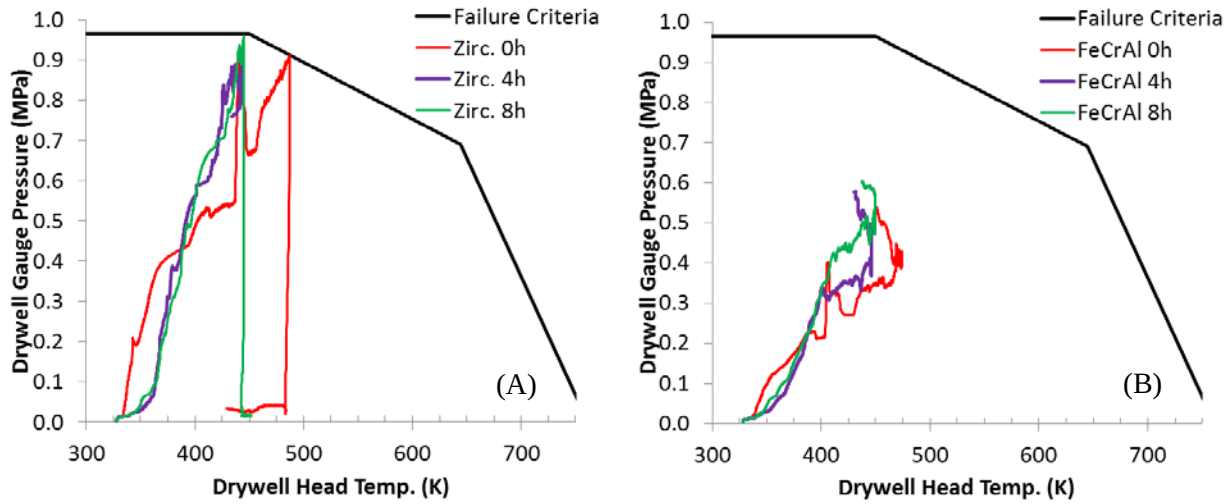

Figure 6. Drywell head loading vs. failure criteria for mitigated Zircaloy (A) and FeCrAl (B) SBO cases.

4. CONCLUSIONS

A range of unmitigated and mitigated station blackout scenarios were simulated to evaluate the potential gains afforded by the FeCrAl ATF concept. Compared to previous simulations [2], this analysis contained updated material properties and an updated plant model, and it used a more recent version of MELCOR. This study also included some required minor MELCOR source code modifications to more accurately model the FeCrAl material. In general, the current analyses results are similar to the previous work [2] and support the same conclusions. In addition, the results are in alignment with similar simulations recently performed for the CPR1000 PWR [6].

In all scenarios analyzed, the FeCrAl ATF concept provided gains over the Zircaloy system being used at this writing. In the unmitigated SBO scenarios, the gains are in the form of delaying the accident progression and decreasing the amount of flammable gases generated. The delays ranged from tens of minutes to a few hours (about 4.5 h) of additional time. Substantially less flammable and non-condensable gasses were generated: 0.6–13.7 tons less by the end of the simulation, depending on the scenario, and the timing of generation was delayed. Given an unmitigated SBO, the FeCrAl ATF concept provides an additional 1–4.4 h of time (depending on scenario) before radionuclide release to the environment, allowing additional time for evacuations.

The results of the mitigated SBO scenarios illustrate the potential benefits of the delayed accident progression and decreased loads on containment. In all three cases analyzed using the FeCrAl ATF concept, the accident was stabilized within 32 h without deflagrations occurring in the building, containment failure, or releases of radionuclides to the environment. In contrast, for two of the cases employing Zircaloy, the containment failed, deflagrations occurred in the reactor building, and radionuclides were released into the environment. Containment was predicted not to fail for one Zircaloy case; however, the loads on containment were predicted to be quite high. The simulations demonstrate the advantage of FeCrAl for enhancing the accident tolerance of a plant by affording an opportunity to mitigate and stabilize a severe accident.

A number of possible improvements and refinements with respect to analyzing FeCrAl were identified during the work:

1. **Scenarios:** A range of SBO severe accidents was analyzed that is representative of higher probability severe accident scenarios [13] and our experience with Fukushima Daiichi [14]; however, there are many other possible severe accident scenarios. Other scenarios, such as unmitigated LOCAs, should be analyzed. In addition, operator response and recovery of water injection (if applicable) were prescribed as the same for both the Zircaloy and the FeCrAl cases analyzed. Differences in operator actions (both on opportunity and success probability) due to the delayed accident progression could be considered in future scenario simulation.

2. **Properties:** Refinement of the thermophysical properties of FeCrAl and FeCrAl oxide, especially for high temperatures, is needed. In addition, the possibility of eutectic formation between FeCrAl and other core components needs to be evaluated. There is ongoing work at ORNL to address these two data needs. These data are needed both for refinement of code predictions and for planning and interpretation of future tests (see next items).

3. **In-Vessel Integral Assessment/Benchmarking:** The severe accident knowledge base and codes (MELCOR) are largely based on the UO_2-Zircaloy fuel system. Oxidation characteristics and balloon-rupture tests have been performed on non-irradiated FeCrAl specimens. However, additional experimental testing is needed to characterize FeCrAl's degradation, reflood, and quench characteristics. Future tests such those in the ORNL's Severe Accident Test Station, KIT's QUENCH facility and/or Halden Reactor (for LOCA / SBO conditions) and/or INL's Transient Reactor Test Facility (for reactivity initiated accidents) could provide the data necessary to (1) provide a validation basis for code predictions and (2) provide empirical confidence in the performance of FeCrAl during a severe accident.

4. **Understanding Ex-Vessel Impact:** Further analysis is need of the behavior of FeCrAl during the ex-vessel portion of the accident progression with respect to its spreading characteristics, MCCI, and the potential for fuel-coolant interactions. These are important phenomena with respect to maintaining containment integrity during severe accidents.

5. **Assembly/System Design:** The potential benefits of FeCrAl during severe accidents should be revisited once a fuel assembly (including any changes to channel box and/or control blade) design has been developed accounting for thermal-hydraulic, neutronic, fuel-performance, and economic considerations.

Although more work is needed, the current analyses suggest that the FeCrAl ATF concept would provide enhanced accident tolerance for a BWR during station blackout severe accidents.

REFERENCES

1. F. Goldner, “Development Strategy for Advanced LWR Fuels with Enhanced Accident Tolerance,” Enhanced Accident Tolerant LWR Fuels National Metrics Workshop, Germantown, MD, October 2012.
2. L. J. Ott, K. R. Robb, D. Wang, “Preliminary assessment of accident-tolerant fuels on LWR performance during normal operation and under DB and BDB accident conditions,” *J. Nuc. Mat.*, **448**(1–3), pp. 520–533 (2014).
3. K. A. Terrani, D. Wang, L. J. Ott, and R. O. Montgomery, “The effect of fuel thermal conductivity on the behavior of LWR cores during loss-of-coolant accidents,” *J. Nuc. Mat.*, **448**(1–3), pp. 512–19 (2014).
4. B. J. Merril and S. M. Bragg-Sitton, “Status Report on Advanced Cladding Modeling Work to Assess Cladding Performance Under Accident Conditions,” INL/EXT-13-30206, September 2013.
5. M. T. Farmer, L. Leibowitz, K. A. Terrani, and K. R. Robb, “Scoping Assessments of ATF Impact on Late Stage Accident Progression Including Molten Core-Concrete Interaction,” *J. Nuc. Mat.*, **448**(1–3), pp.534–40 (2014).
6. X. Wu, et al, “Preliminary Safety Analysis of PWR with Accident-Tolerant Fuel during Severe Accident Conditions,” *Annals of Nuc. Energy*, **80**, pp.1–13 (2015).
7. J. H. Chun, S. W. Lim, B. D. Chung, W. J. Lee, “Safety evaluation of accident-tolerant FCM fuel core with SiC-coated zircaloy cladding for design-basis-accident and beyond DBAs,” *Nuclear Engineering and Design*, **289**, pp. 287–95 (2015).
8. S. Bragg-Sitton, B. Merrill, M. Teague, L. Ott, K. Robb, M. Farmer, M. Billone, R. Montgomery, M. Todosow, and C. Stanek, “Advanced Fuels Campaign Light Water Reactor Accident Tolerant Fuel Performance Metrics,” INL/EXT-13-29957, FCRD-FUEL-2013-000264, February 2014.
9. K. A. Terrani, S. J. Zinkle, L. L. Snead, “Advanced Oxidation Resistant Iron-Based Alloys for LWR Fuel Cladding,” *J. Nuc. Mat.* **448**(1–3), pp. 420–35 (2014).
10. B. A. Pint et al., “High temperature oxidation of fuel cladding candidate materials in steam-hydrogen environments,” *J. Nuc. Mat.*, **440**, pp. 420–27 (2013).
11. Sandia National Laboratories, MELCOR Computer Code Manuals, Version 1.8.5, NUREG/CR-6119, Rev. 2, October 2000.
12. US Nuclear Regulatory Commission, “State-of-the-Art Reactor Consequence Analyses Project; Volume 1: Peach Bottom Integrated Analysis,” NUREG/CR-7110, Vol. 1, January 2012.
13. US Nuclear Regulatory Commission, “Severe accident risks: an assessment for five US nuclear power plants, NUREG-1150,” US Nuclear Regulatory Commission, Washington, DC, 1990.
14. Nuclear Emergency Response Headquarters, Government of Japan, “Report of Japanese Government to the IAEA Ministerial Conference on Nuclear Safety — The Accident at TEPCO’s Fukushima Nuclear Power Stations,” June 2011.
15. Sandia National Laboratories, MELCOR Computer Code Manuals, Version 1.8.6, NUREG/CR-6119, Rev. 3, September 2005.
16. Sandia National Laboratories, MELCOR Computer Code Manuals, Version 2.1, NUREG/CR-6119, Rev. 4, September 2008, Draft.
17. K. R. Robb, “Updated Peach Bottom Model for MELCOR 1.8.6: Description and Comparisons,” ORNL/TM-2014/207, September 2014.
18. L. J. Ott, “Advanced Severe Accident Response Models for BWR Application,” *J. Nuc. Mat.* **115**, pp. 289–303 (1989).
19. B. A. Pint, K. A. Terrani, Y. Yamamoto, and L. L. Snead, “Material Selection for Accident Tolerant Fuel Cladding,” *Metallurgical and Materials Transactions E*, submitted, 2014.
20. J. J. Powers, N. M. George, A. Worrall, and K. A. Terrani, “Reactor Physics Assessment of Alternate Cladding Materials,” *Transactions of the 2014 Water Reactor Fuel Performance Meeting*

/ Top Fuel / LWR Fuel Performance Meeting (WRFPM2014/TopFuel 2014), Sendai, Japan, September 14–17, 2014.
21. N. M. George, K. A. Terrani, J. J. Powers, A. Worrall, and G. I. Maldonado, "Neutronic Analysis of Candidate Accident-Tolerant Cladding Concepts in Pressurized Water Reactors," *Annals of N. E.*, **75**, 703–12 (2015).
22. N. M. George, J. J. Powers, G. I. Maldonado, K. A. Terrani, and A. Worrall, "Neutronic Analysis of Candidate Accident-tolerant Cladding Concepts in Light Water Reactors," Transactions of the American Nuclear Society, 111 (2014) 1363–66.
23. N. M. George, J. J. Powers, G. I. Maldonado, A. Worrall, and K. A. Terrani, "Demonstration of a Full-core Reactivity Equivalence for FeCrAl Enhanced Accident Tolerant Fuel in BWRs," *Proc. of Advances in Nuclear Fuel Management V (ANFM V)*, Hilton Head Island, South Carolina, USA, March 29 – April 1, 2015.
24. K. R. Robb, M. T. Farmer, M. W. Francis, "Ex-Vessel Core Melt Modeling Comparison between MELTSPREAD-CORQUENCH and MELCOR 2.1," ORNL/TM-2014/1, March 2014.
25. J. Rempe, M. Farmer, M. Corradini, L. Ott, R. Gauntt, D. Powers, "Revisiting Insights from Three Mile Island Unit 2 Postaccident Examinations and Evaluations in View of the Fukushima Daiichi Accident," *J. Nuc. Sci. and Eng.* **172**, pp. 223–48 (2012).

Appendix A: MELCOR Parametric Study

A simple parametric study in MELCOR was attempted. The goal of the study was to identify which fuel, cladding, and structure property changes provide the best potential improvements for delaying or mitigating severe accidents.

The method employed for the parametric study was to first define a base case, then define the parameters and ranges over which they would be varied, followed by MELCOR simulations where only one parameter in the base case would be perturbed. The results for key figures of merit would be recorded, and, finally, the results were analyzed to quantify sensitivities.

A long-term station blackout was simulated for the Peach Bottom BWR/4 with a Mark I containment. AC electrical power was assumed to be lost at reactor shutdown; however, DC power from batteries was assumed to last 8 h. The simulation is specified to end 32 h after reactor shutdown. The fuel was specified as UO_2, and the cladding was Zircaloy. MELCOR version 1.8.6(.4073), as compiled by Sandia National Laboratories, was used.

The test matrix for the parametric study is summarized in Table A.1.

The integral nature of severe accidents coupled with binary (on/off) phenomena (e.g., bottom head failure, containment failure, deflagrations); time dependence (e.g., decay heat, failure modes); strong history effect (i.e., past failures and phenomena affect future); and regime-dependent phenomena (e.g., flow and heat transfer correlations) compounds the difficulty in interpreting results. A small change in an initial condition (e.g., fuel and/or cladding properties) can result in major differences in the accident progression timing. Due to these effects, many of the trends from the parametric study were irregular and not easily interpreted. After performing preliminary analysis, it was determined that a significant amount of effort would be required to properly interpret the results. For this reason, further parametric analysis study was not pursued in FY 2014.

Table A.1. Parametric study cases.

Category	Parameter	Variation Type
Radionuclide Initial Distribution and Release	Cladding Rupture Temperature	-100 K to Rupture Temperature
		+100 K to Rupture Temperature
		+200 K to Rupture Temperature
	Radionuclide Diffusion Coefficient in Fuel	0.100× Diffusion Coefficient
		0.010× Diffusion Coefficient
		0.001× Diffusion Coefficient
	Initial Radionuclide Distribution between Fuel and Gap	0.0× Initial RN in Gap
		0.5× Initial RN in Gap
	RN Initial Distribution and Diff. Coeff.	0.100× D - 0 RN in Gap
		0.010× D - 0 RN in Gap
		0.001× D - 0 RN in Gap
Fuel/Cladding Failure Mechanisms	Cladding Failure due to Time at Temperature	1.1× Allowed Time at Temperature
		0.9× Allowed Time at Temperature
		10.0× Allowed Time at High Temp.
		20.0× Allowed Time at High Temp.
	Melting Temperature	+200 K to Zr Melting Temp.
		+200 K to Clad & Fuel Melt Temp.
Cladding Oxidation Kinetics	Cladding Oxidation Kinetics	0.100× Zr Oxidation Rate
		0.010× Zr Oxidation Rate
		0.001× Zr Oxidation Rate
Fuel/Cladding Thermal Conductivity	Cladding Thermal Conductivity	1.1× Clad Thermal Conductivity
		0.9× Clad Thermal Conductivity
Assembly Design	Cladding Mass	0.90× Cladding Mass
		0.75× Cladding Mass